

Thickness evolution of the Scandinavian Ice Sheet during the Late Weichselian in Nordfjord, western Norway: evidence from ice-flow modeling

CORNELIA WINGUTH, DAVID M. MICKELSON, EILIV LARSEN, JESSICA R. DARTER, CAROLYN A. MOELLER AND KNUT STALSBERG

BOREAS



Winguth, C., Mickelson, D. M., Larsen, E., Darter, J. R., Moeller, C. A. & Stalsberg, K. 2005 (May): Thickness evolution of the Scandinavian Ice Sheet during the Late Weichselian in Nordfjord, western Norway: evidence from ice-flow modeling. *Boreas*, Vol. 34, pp. 176–185. Oslo. ISSN 0300-9483.

Results from experiments with a two-dimensional ice-flow model, applied along a west–east transect in western Norway, provide new constraints on the thickness evolution of the Scandinavian Ice Sheet throughout the Late Weichselian glaciation and deglaciation. Investigations took place along an E–W flowline of the former ice sheet at *c.* 62°N, from the modern glacier Jostedalbreen, through the Nordfjord, and across the continental shelf. A paleoclimate record from Kråkenes, which is located directly at the flowline, provides temperature and precipitation information for the time between 13 800 and 9200 cal. yr BP. LGM climate conditions for the study area are estimated from various GCM studies. The GISP2 $\delta^{18}\text{O}$ record has been tuned to the local data in order to provide a continuous temperature record as input for time-transgressive model runs. The results of all experiments suggest that the ice did not cover the highest mountain peaks in this area, and that nunataks persisted throughout the Late Weichselian glaciation. These findings are in contrast to results from many previous model studies and other ice-sheet reconstructions, but agree well with minimum thickness estimates from cosmogenic dating and with vertical ice limits inferred from lower block field boundaries and trimlines.

Cornelia Winguth (e-mail: cwinguth@facstaff.wisc.edu), Department of Geology and Geophysics, University of Wisconsin, 1215 W. Dayton St., Madison, WI 53706, USA, and Department of Atmospheric and Oceanic Sciences, University of Wisconsin, 1225 W. Dayton St., Madison, WI 53706, USA; David M. Mickelson (e-mail: davem@geology.wisc.edu), Jessica R. Darter (e-mail: jdarter@geology.wisc.edu), Carolyn A. Moeller (e-mail: moeller@geology.wisc.edu), Department of Geology and Geophysics, University of Wisconsin, 1215 W. Dayton St., Madison, WI 53706, USA; Eiliv Larsen (e-mail: Eiliv.Larsen@ngu.no), Knut Stalsberg (e-mail: Knut-Stalsberg@ngu.no), Geological Survey of Norway, Leiv Eirikssons v. 39, NO-7491 Trondheim, Norway; received 5th April 2004, accepted 8th December 2004.

The thickness of the Scandinavian Ice Sheet at the Last Glacial Maximum (LGM) has long been disputed, especially in the mountainous areas of southwestern Norway, due to divergent geologic evidence (e.g. Nesje *et al.* 1987; Follestad 1990; Larsen *et al.* 1995; Brook *et al.* 1996). It is essential, however, to be able to reconstruct ice thickness in addition to ice extent, because the volume and height of the ice sheet strongly influenced global sea level and ocean and atmospheric circulation, and are therefore important boundary conditions for paleoclimate modeling (e.g. Manabe & Broccoli 1985; Peltier 1994; Kutzbach *et al.* 1998; Clark *et al.* 1999; Lambeck *et al.* 2000). Landforms and the sediment record provide good constraints on the maximum lateral extent of the Scandinavian Ice Sheet (e.g. Andersen 1981; Svendsen *et al.* 1999; Larsen *et al.* 1999; Sejrup *et al.* 2000), but its vertical extent and surface profile are more difficult to establish. For example, botanists postulated the existence of ice-free regions in western and northern Norway at the LGM, allowing the survival of endemic plant and animal species (for review, see Nesje *et al.* 1988). This is

supported by geomorphic evidence, including steep-sided peaks (regarded as nunataks), cirque topography, and summit block fields produced by *in situ* rock weathering for a period of time longer than the Holocene. The lower boundary of autochthonous block fields gradually decreases in elevation from *c.* 2000 m a.s.l. at the central mountain range of southern Norway to 500–600 m a.s.l. at the coast (Nesje *et al.* 1988). Nesje *et al.* (1987, 1988) and Nesje & Dahl (1990) interpret this trimline as the upper limit of the Late Weichselian ice sheet. This conclusion was strengthened by cosmogenic nuclide exposure ages of >55 ka for summit regions in western Norway (at Skåla) and 26–21 ka below the trimline (Brook *et al.* 1996). The ice sheet inferred from the above evidence by Nesje *et al.* (1988) is relatively thin and controlled by the regional topographical features in southern Norway. Its ice divide during the maximum glaciation was located close to the present-day main surface water divide in southwestern Norway.

A contrasting picture results from other methods of ice-sheet reconstruction including numerical modeling,

preconsolidation tests and information from till fabrics and striation patterns. Many previously published reconstructions predict a Scandinavian Ice Sheet that continued to rise toward the east of the modern watershed at the LGM (e.g. Oerlemans 1981; Hughes *et al.* 1981; Boulton *et al.* 1985; Boulton & Payne 1994; Huybrechts & T'siobbel 1995; Boulton *et al.* 2001; Siegert *et al.* 2001). Follestad (1990) studied till fabrics and striation patterns in the Nordmøre region of western Norway and deduced ice movement that was independent of the local topography, suggesting an ice surface above all mountain summits. Furthermore, he found erratic blocks and till in some block fields, indicating that the block fields could have been covered by ice without being eroded. The lower boundary of the block fields was attributed to a minor ice readvance after the LGM. Another possible explanation for the trimlines observed in the field, which are often interpreted as weathering boundaries, is that they represent englacial thermal boundaries, marking the transition from thinner, non-erosive, cold-based ice covering the ridge tops to thicker, erosive, warm-based ice in the valleys (e.g. Sollid & Sørbel 1994). Basal thermal zonation has been inferred for many areas of the Scandinavian Ice Sheet (e.g. Kleman *et al.* 1999; Kleman & Hättestrand 1999). Preconsolidation tests performed on sediments overridden by LGM ice indicated an ice surface at least ~ 400 m above the upper trimline in western Norway (Larsen *et al.* 1995), suggesting a complete ice cover of the area. However, new preconsolidation tests on samples from the same site (Skorgedalen, western Norway, at *c.* 63°N), using the constant strain rate method rather than incremental loading, indicate substantially lower minimum ice thickness close to the elevation of the trimline (Hildreth 2001). Based on roughness measurements at Skåla, in the Nordfjord area, which indicate the degree of rock surface weathering, McCarroll & Nesje (1993) concluded that the ice during the LGM either extended over all summits, but was cold-based and therefore did not erode the bedrock, or its maximum vertical limit was even lower than previously suggested (at *c.* 1350 m a.s.l.).

Using a time-dependent, numerical model with a relatively high resolution (10–11 km) for simulation of the development of the Scandinavian Ice Sheet along a flowline in southwestern Norway, we seek to contribute new insights into this still unresolved problem.

Study area

We use a flowline of *c.* 311 km length for our ice-flow model experiments. It starts close to the present-day water divide at Jostedalbreen, a modern glacier, and runs through Nordfjord, onto the shelf and beyond the shelf edge (Fig. 1).

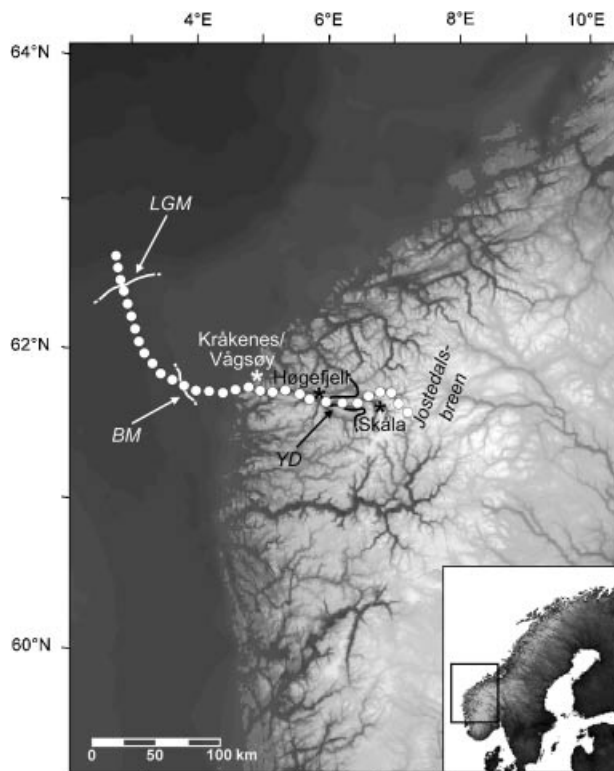


Fig. 1. Study area in southwestern Norway. The flowline used for the ice-flow model experiments is marked with white dots. It starts at the present-day glacier of Jostedalbreen, runs through the Nordfjord and ends offshore at 603 m water depth. Skåla, Høgefjell and Vågsøy are locations where cosmogenic dates exist that are used for comparison with model results. Ice extents mentioned in the text are marked: LGM = Last Glacial Maximum, BM = Bremanger Moraine, YD = Younger Dryas.

The bedrock in the Nordfjord area consists mainly of Precambrian gneisses and granites (Kildal 1970; Lutro 1997). Cambro-Silurian rocks, mainly phyllite and mica schist, dominate in inner Nordfjord (Fareth 1987; Nesje *et al.* 1988). Narrow valleys in western Norway were first cut into the bedrock as a result of Tertiary uplift (Donner 1995, and references therein). Extensive erosion during several Quaternary glaciations (e.g. Nesje *et al.* 1992) has led to the broadening and deepening of the valleys, and hence to the excavation of the fjord, fjord lakes, and valleys. Their orientation mainly follows the east–west trend of the bedrock structures in the Nordfjord area (Fareth 1987). The proximal end of Nordfjord branches into several valleys, some of which lead to outlet glaciers from Jostedalbreen. Apart from these valleys, the topography in the Nordfjord region is dominated by smooth mountain tops, bordered by steep cliffs, that represent remnants of a planation surface developed close to sea level during the Mesozoic and dissected following uplift in the Cenozoic (e.g. Riis 1996). The summits around Nordfjord descend from 1800–2000 m a.s.l. at

Jostedalbreen to 400–600 m a.s.l. at the coast (Nesje *et al.* 1987). The sedimentary cover in the mountain area is sparse. Most of the till derived from the Weichselian glaciations has been deposited in ice-marginal zones and below the marine limit in the main valleys of the Nordfjord system.

Model description

Model outline

We use a two-dimensional, time-dependent, thermo-mechanically coupled finite-element ice-flow model, which has already been applied successfully in several studies of the Laurentide Ice Sheet (e.g. Cutler *et al.* 2000, 2001; Winguth *et al.* 2004). Horizontal ice-flow velocity is composed of deformation and sliding velocity, the latter occurring only if the temperature at the ice base is at the pressure melting point at two or more neighboring nodes. Glen's flow law is used for ice deformation; sliding parameterization follows Payne (1995) and Greve & MacAyeal (1996). Sediment deformation is not treated separately. By applying appropriate sliding parameters in the sliding law, 'hard' bedrock and 'soft' sediments influence basal motion differently, with the latter facilitating fast ice flow (Clark *et al.* 1999). Permafrost development and isostatic adjustments through time are incorporated in the model. A detailed description of these model features is given in Cutler *et al.* (2000, 2001) and Parizek (2000). The model includes flow divergence or convergence and accounts for side-wall friction in the fjords by application of a shape factor in the calculation of horizontal velocity distribution, which varies along the flowline, following the approach by, for example, Paterson (1994) and Hooke (1998). Calving rate in the model is dependent on water depth at the ice front, using the relationship established by Pelto & Warren (1991) from the analysis of 22 tidewater glaciers.

Model input

Model values along the flowline are calculated at 31 nodes (with a horizontal resolution of 10–11 km) and for 25 ice and 31 bedrock layers (down to a depth of 830 m below the surface). The timestep of the runs was set to 10 years. Digital topographic data as well as sediment thickness information in the fjord was provided by the Geological Survey of Norway. Sediment thicknesses for the offshore region are estimated from a seismic study about 150 km farther south by Sejrup *et al.* (1991). Accurate data on former sediment thickness and distribution is not available, so we use the present-day sediment thickness along the flowline. We assume that a similar sediment distribution existed before the last ice advance and that this sediment was partly removed and replaced by new sediment during

and after deglaciation. Geothermal heat flux values, applied at the base of the model domain, increase along the flowline from approximately 45 to 60 mW m⁻² (Kukkonen *et al.* 1998; see also references therein). Local sea-level changes at the ice margin are calculated by inferring global sea level changes from the SPEC-MAP $\delta^{18}\text{O}$ record (Imbrie *et al.* 1984) and taking into account isostatic adjustments.

The most important parameters driving the model are temperature and precipitation. Present-day climate information for our study area has been provided by the Norwegian Meteorological Institute (Ø. Nordli, pers. comm. 2002). The recent mean annual temperature at Kråkenes is about 7°C, and mean annual precipitation about 1500 mm. The LGM range for southwestern Norway is about -2 to -10°C for mean annual temperature and 500 to 1200 mm for annual precipitation, based on output from global and regional climate model studies (Kutzbach *et al.* 1998; Ganopolski *et al.* 1998; Shin *et al.* 2003; R. Bryson, pers. comm. 2001). A regional climate model nested into an AGCM yields temperature and precipitation values over Europe for the time of the Younger Dryas (Renssen *et al.* 2001). It suggests winter temperatures about 20°C cooler than today and summer about 5–10°C cooler than today. Precipitation results from Renssen *et al.* (2001) were c. 3–5 mm/day in winter and c. 2–3 mm/day in summer.

A paleoclimate record from fossil plants and animals in lake sediments at Kråkenes, which is located on Vågsøy Island just north of our flowline, yields local temperature and precipitation information for the time of 13 800 to 9200 cal. yr BP (Birks *et al.* 2000). We use the GISP2 $\delta^{18}\text{O}$ record (Grootes & Stuiver 1997) in conjunction with this information to provide us with a longer time series of temperature. Back to 40 ka BP, the GISP2 ages rely on layer counting and are regarded as fairly reliable (Cuffey & Clow 1997). The GISP2 record was adjusted to the local paleotemperature record at Kråkenes by modifying the amplitude and adding a constant. The converted record was then used directly as paleotemperature input. A similar approach has successfully been used for a deglaciation modeling study of the southern Laurentide Ice Sheet (Winguth *et al.* 2004). The input temperature varies along the flowline using an elevation lapse rate of 0.0059°C/m, based on the present-day temperature gradient in the area. Dahl & Nesje (1992) used a similar value in their calculations of former ELA in the Nordfjord area. The baseline precipitation (at sea level) is adjusted for earlier times using a 'precipitation factor' and also varies along the flowline based on the modern trend, with precipitation increasing from the coast to a maximum in the coastal mountains (up to about 4000 mm/year; Ø. Nordli, pers. comm. 2002).

Many studies support our approach of using a Greenland $\delta^{18}\text{O}$ record as a proxy of paleotemperature for the area of western Norway. For example, Bond *et al.* (1993) inferred from sediment cores in the North

Table 1. List of experiments. Experiment 15 represents the 'standard' experiment. Sliding is parameterized after Clark *et al.* (1999) and calving is set up using the relationship established by Pelto & Warren (1991). For explanation of other parameters, see text.

Experiment	Temperature parameterization	Precipitation factor	Other parameters
06	$f=1.2$ $c=46$	1.0–0.765 (21 ka BP)–1.0	see Experiment 15
08	$f=1.3$ $c=49.4$	1.0–0.765 (21 ka BP)–1.0	see Experiment 15
10	$f=1.4$ $c=53.5$	1.0–0.765 (21 ka BP)–1.0	see Experiment 15
12	$f=1.3$ $c=49.4$	1.0–0.6 (21 ka BP)–1.0	see Experiment 15
13	$f=1.3$ $c=49.4$	1.0–0.5 (21 ka BP)–1.0	see Experiment 15
14	$f=1.3$ $c=49.4$	1.0–0.4 (21 ka BP)–1.0	see Experiment 15
15 'Standard'	$f=1.3$ $c=49.4$	1.0–0.6 (21 ka BP)– 0.85 (12 ka BP)–1.0	Factor in calving equation: 8.33 Sliding parameter: $2.0 * 10^{-3} \text{ m yr}^{-1} \text{ Pa}^{-1}$ Ice extent at beginning: 1/20 of flowline
16	$f=1.3$ $c=49.4$	1.0–0.6 (21 ka BP)– 0.85 (12 ka BP)–1.0	Sliding parameter: $5.0 * 10^{-3} \text{ m yr}^{-1} \text{ Pa}^{-1}$, otherwise like Experiment 15
17	$f=1.3$ $c=49.4$	1.0–0.6 (21 ka BP)– 0.85 (12 ka BP)–1.0	No ice extent at beginning, otherwise like Experiment 15
18	$f=1.3$ $c=49.4$	1.0–0.6 (21 ka BP)– 0.85 (12 ka BP)–1.0	Factor in calving equation: 18, otherwise like Experiment 15
19	$f=1.3$ $c=49.4$	1.0–0.6 (21 ka BP)– 0.85 (12 ka BP)–1.0	Flowline extended to east by 57 km (with adjusted precipitation elevation gradient), otherwise like Experiment 15

Atlantic that shifts in sea surface temperatures must have been in phase with air temperature changes above Greenland, and that rates of change in ocean temperatures must have been nearly the same as in the ice cores. A sediment core from the Norwegian Sea also reveals climate changes in phase with air temperature changes over Greenland (Fronval *et al.* 1995). A high-resolution record of planktonic fauna from the Norwegian Channel covering the past 16 ka shows that timing and rate of change fit in detail the isotope record of the GRIP core, suggesting that the Greenland ice core data reflect northwest European climate in great detail (Hafliðason *et al.* 1995). And, finally, high-resolution pollen stratigraphy from southern Finland demonstrates many similarities with the Greenland $\delta^{18}\text{O}$ records (Heikkilä & Seppä 2003).

Experiments

Experiments with time-transgressive climate input have been carried out for the time of 40 ka BP to today, with

the first 8 ka being regarded as model spin-up time. The sensitivity of the model to a possible range of paleoclimate variability, to initial ice coverage, to variations in calving and in sliding parameterization as well as to an assumed ice divide location farther east (at Jotunheimen) has been explored. Known ice extent along the flowline through time is used for model validation. The experiment that yielded the best results in terms of ice extent through time (Experiment 15) will be referred to as the 'standard' experiment. Various experiments and their input parameters are listed in Table 1.

Paleotemperature input has been varied using a range of factors f and constants c in the following equation that converts GISP2 $\delta^{18}\text{O}$ data into temperature t at Kråkenes:

$$t = f * \delta^{18}\text{O}_{\text{GISP}} + c [^{\circ}\text{C}]$$

Figure 2A illustrates the mean annual temperature at Kråkenes generated by using the adjusted GISP2 $\delta^{18}\text{O}$ record in our standard model run together with the Kråkenes record that has been used for modification of

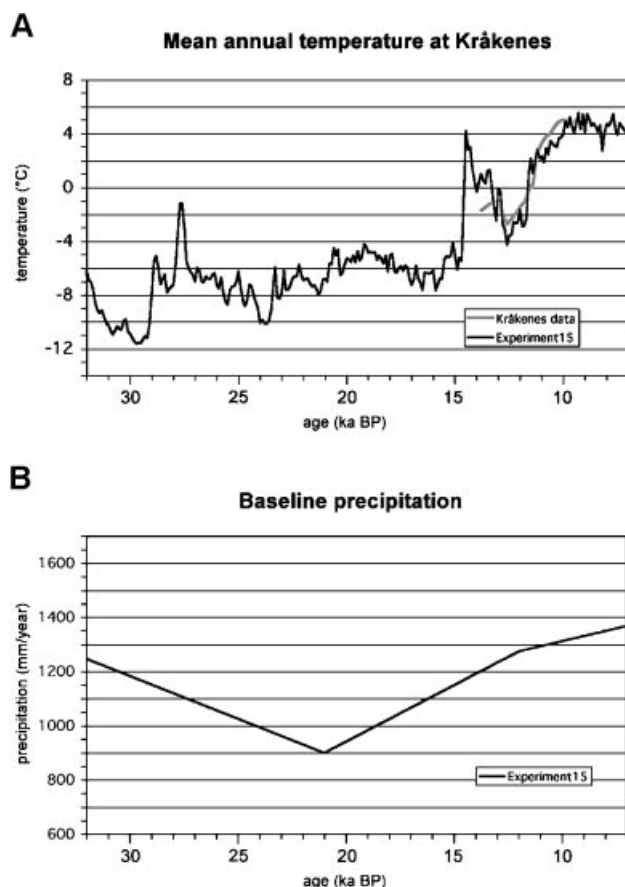


Fig. 2. A. Modeled input temperature through time at the location of Kråkenes as derived from the GISP2 $\delta^{18}\text{O}$ record in comparison with paleotemperature data from Kråkenes (Birks *et al.* 2000). B. Baseline precipitation input as used in the standard experiment.

the GISP2 curve. The resulting temperature of *c.* -12°C during maximum ice extent and *c.* -10°C around 24 ka BP lies at the lower end of the range suggested by GCM model studies.

Precipitation input was varied by using a precipitation factor of 0.4 to 0.765 for the time of 21 ka BP (corresponding to the LGM) and assuming present-day precipitation conditions with a precipitation factor of 1.0 at the beginning (at 40 ka BP) and at the end of the model runs. The precipitation factor decreases or increases linearly over time between the different values, yielding a range of 0.66 to 0.87 for the time of 12 ka BP (corresponding to the Younger Dryas). This corresponds well with the approximate mean precipitation range of 60% to 97% of today's precipitation simulated for the Younger Dryas by Renssen *et al.* (2001). For some of the experiments, including the standard experiment 15, the precipitation factor at 12 ka BP was set to 0.85. In this case, precipitation factors through time were interpolated between the values at the beginning, at 21 ka BP, at 12 ka and at the end of the run (see precipitation factor in Table 1). Figure 2B shows the baseline precipitation input through time

for the standard model run. In the case of a flowline extension to the east (Experiment 19), the precipitation elevation gradient of 0.00125/m used in the other runs has been adjusted to 0.001/m in order to distribute the precipitation along the longer flowline and not to exceed the maximum of 4000 mm/year.

Discussion of model results

Lateral ice extents through time

The extent of deglaciation during the last interstadial (the Ålesund interstadial) is uncertain (Larsen *et al.* 1995). Subsequent ice build-up to the Late Weichselian glacial maximum happened very quickly (probably within 3000–4000 years; Larsen *et al.* 1987), and the maximum Weichselian glaciation occurred between 29.4 and 22 ^{14}C ka BP (Sejrup *et al.* 1994). At this time, the ice margin was located at the continental shelf edge (e.g. Andersen 1981; Sejrup *et al.* 2000; Boulton *et al.* 2001; Nygård *et al.* 2004). A retreat at least to within the present coastline during the Hamnsund interstadial was followed by the Tampen readvance onto the shelf around 19 ^{14}C ka BP (Sejrup *et al.* 1994, 2000; Valen *et al.* 1996). Nygård *et al.* (2004) identified the Bremanger event in our study area, with an age between 15 and 13.3 ^{14}C ka BP, which corresponds to the later part of the Tampen readvance. During the Davik stadial (at *c.* 13 ^{14}C ka BP), the ice margin was probably situated in the outer fjord areas, and by 12 ^{14}C ka BP it had retreated to the head of the fjord. The Nor stadial (corresponding to the latter half of the Younger Dryas, around 10.5 ^{14}C ka BP) is a prominent glacial phase represented by a moraine in the mid-Nordfjord area (Fareth 1987). Glacier retreat following the Nor stadial probably occurred very rapidly, because no ice-marginal deposits younger than the Nor moraines are found in the main fjord.

Figure 3 displays the ice extent along the flowline through time created by the standard model run (Experiment 15, see Table 1). Ice extents that have been identified in the field are shown for comparison and are used for model validation. Calibrated ^{14}C ages of events discussed above are used here for easier comparison with model output (Table 2). The combination of climate input parameters used in this experiment, which all fall within the probable range of temperature and precipitation given by GCM output and local data, yields the ice extent that best fits the field record. The maximum ice extent is reached between 31 and 29 model ka BP; then the ice retreats almost to the coastline, corresponding to the Hamnsund interstadial. A minor subsequent readvance reaches approximately the Tampen ice extent (between 24 and 23 model ka BP). During the time corresponding to Nygård *et al.*'s (2004) Bremanger event, the modeled ice margin has already retreated close to the coastline

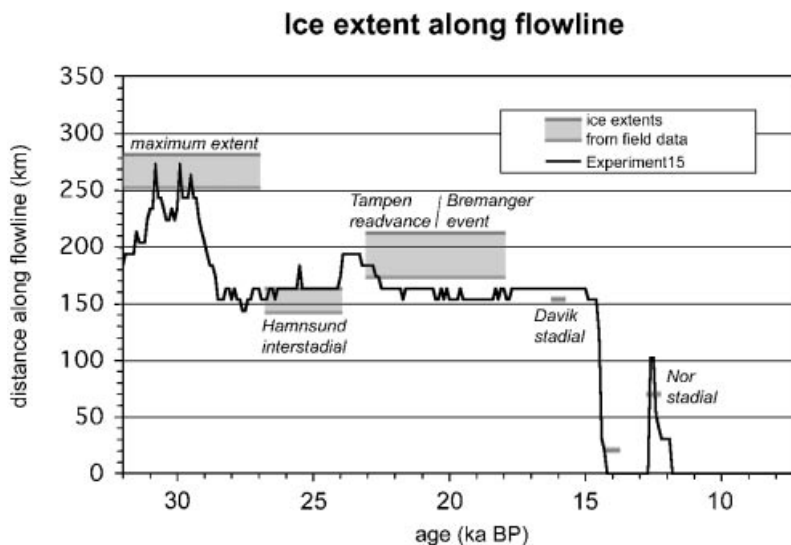


Fig. 3. Ice extent along the flowline through time from standard experiment. Also marked are ice extents derived from field evidence for comparison with model results.

again. Subsequent deglaciation in the model starts at *c.* 15 model ka BP and occurs very rapidly. The model produces a minor readvance at 12.6 model ka BP, to a location a little farther seaward than the Younger Dryas extent identified in the Nordfjord.

Only a combination of relatively low LGM temperature, relatively low LGM precipitation and relatively high Younger Dryas precipitation with respect to paleoclimate output from GCMs yields reasonable ice extents for the last 32 000 years. Decreasing the amplitude of the input temperature curve (by changing a combination of *f* and *c*, e.g. Experiment 06) produces no ice readvance around 12 ka BP, even when using a high precipitation factor. Increasing the amplitude of the input temperature curve (e.g. Experiment 10) yields a complete melting of the ice between 27 and 26 model ka BP and an ice extent about 50 km too far along the flowline for the extent corresponding to the Tampen readvance. Comparison of different precipitation factors for the LGM (Experiments 12–14) shows that maximum ice extent is best represented when using relatively low LGM precipitation (60%, as in Experiment 12). Going down to 40% (Experiment 14), however, results in complete ice melting by 26.7 model ka BP and no further ice development. In order to

achieve an ice readvance representing the Younger Dryas extent, it is necessary to increase precipitation at that time to more than 80% of today's precipitation, as has been done in Experiment 15, in contrast to Experiment 12. This result is in good agreement with findings by Larsen & Stalsberg (2004), who concluded that relatively high accumulation during the Younger Dryas period was necessary to form and maintain the cirque moraine that existed close to Kråkenes at this time. Changing the sliding parameter (Experiment 16, see Table 1) to a higher value within the reasonable range explored by Cutler *et al.* (2000) has no important impact on ice extent. The same is true for completely removing the ice coverage along the flowline (since the extent of deglaciation at the last interglacial is not exactly known) at the beginning of the run (Experiment 17). Significantly increasing calving rate (based on the fact that polar as well as temperate glaciers were used by Pelto & Warren (1991) in order to establish the relationship, which might underestimate calving of the latter) leads to complete ice retreat by 27 model ka BP. Extending the flowline to the east (Experiment 19) leads to a significant ice retreat between *c.* 28 and 26 model ka, but otherwise produces an ice extent pattern very similar to the standard run.

Table 2. ^{14}C ages of glacial events recorded in the geologic record and their corresponding calibrated ages (Stuiver *et al.* 1998; Beck *et al.* 2001).

Event	^{14}C ka BP	cal. ka BP
Last Glacial Maximum	Between 29.4 and ~22	Between ~34.5 and ~27
Hamnsund Interstadial	Between ~22 and ~19	Between ~27 and ~24
Tampen Readvance	Between ~19 and ~14	Between ~24 and ~17.5
Bremanger Event	Between ~15 and ~13.3	Between ~18.5 and ~16.5
Davik Stadial	Around 13	Around 16
Nor Stadial	Around 10.5	Around 12.5

Overall, the model reproduces the known ice margins through time reasonably well in the standard experiment. The fact that the model fails to generate the Bremanger readvance might indicate that precipitation is underestimated in the model for this time. Another possible explanation is that not only climate deterioration, but also glacier surging (which is not incorporated in the current model) played an important role at this time.

Ice thickness

Ice thickness profiles generated by our standard model run (Experiment 15) are shown in Fig. 4 for two time slices: 29.85 model ka BP (corresponding to the maximum extent during the last glaciation) and 12.6 model ka BP (corresponding to the last readvance during the Younger Dryas). The close-by locations of Skåla, Høgefjell and Vågsøy, where results from field studies are available for comparison to our standard model results, are projected onto the flowline, and the known trimlines are marked.

Brook *et al.* (1996 and in prep.) determined ^{10}Be ages of bedrock from vertical transects at several locations in the Nordfjord area, among them Vågsøy and Skåla. At Skåla (summit elevation 1880 m), a sequence of samples has ages that decrease from *c.* 26–31 ka BP at ~ 1500 – 1700 m a.s.l. to *c.* 11–13 ka BP at 1000–1200 m a.s.l., covering the main part of the deglaciation of this area. The data agree well with our maximum surface elevation values of 1612 m a.s.l. at Skåla for 29.85 model ka BP (Fig. 4). For the times of, for example, 21, 15 and 12.6 model ka BP, we obtain surface elevation values of 1271, 1232 and 997 m a.s.l., respectively, showing a similar trend as Brook *et al.*'s data. The highest trimline identified in the area, which borders the summit block field, has an elevation of *c.* 1560 m a.s.l.; another trimline is evident at 1350 m a.s.l., and the lowest trimline, which has been interpreted as the Younger Dryas ice limit, is positioned at *c.* 1100 m a.s.l. (Nesje *et al.* 1988; McCarroll & Nesje 1993). While a thin, cold-based ice sheet covering mountain peaks in the area and protecting the highest elevations from erosion cannot be ruled out by cosmogenic results alone (Brook *et al.* 1996), comparison with our model results indicates that the highest trimline most likely represents the maximum ice thickness during the last glaciation. This is also in agreement with Nesje & Dahl's (1990) argument against the regionally consistent weathering boundary being of thermal origin, since englacial isotherms are commonly not parallel to the ice sheet surface over wide areas. The trimline at 1350 m a.s.l. is close to the modeled vertical ice limit that has been correlated with the Tampen readvance. The modeled ice surface elevation for the readvance at 12.6 ka BP (that has been correlated with the Younger Dryas event) is about 100 m lower than the lowest trimline.

New cosmogenic data from Høgefjell (mid-Nordfjord) at elevations of *c.* 1000 m a.s.l. yield exposure ages of ~ 15 – 24 ka BP (H. Linge, pers. comm. 2004). Our results are in relatively good agreement with these data, showing a maximum ice surface elevation of 1349 m a.s.l. for this location, and ice retreat to 992 m a.s.l. by 24 ka BP and 856 m a.s.l. by 15 ka BP.

At Vågsøy, a coastal site, bedrock exposure ages for altitudes between *c.* 450 and 200 m a.s.l. decrease from *c.* 17–18 ka BP to *c.* 12–15 ka BP (Brook *et al.* in prep.). Our corresponding thickness values for this site are somewhat higher, with 590 m a.s.l. at 17 ka BP, decreasing to 537 m a.s.l. at 15 ka BP. After that, rapid deglaciation takes place in the model, leaving the coastal area ice-free by 14.5 ka BP. No surging mechanism is included in the model at the present stage, but probably a water film at the ice bottom developed (Moeller 2004.) that could have led to very fast ice movement. This would have impacted the ice surface profile, especially near its outer edge, and might explain the discrepancies between the results from cosmogenic dating and from our ice-flow model experiments.

Ice-sheet thickness is one of the most important unresolved issues necessary for modeling the Last Glacial Maximum climate. Ice sheets are large topographic features that create anomalies in albedo and radiation balance, and represent important freshwater reservoirs. Therefore, ice sheets have an important influence on climate, either directly by displacing the winter jet stream, by cooling the air over and downwind of the ice sheets, and by reorganizing storm tracks, or indirectly by influencing the ocean circulation through freshwater releases and by changing the sea level (Clark *et al.* 1999). Our inferred ice sheet along the flowline is thinner than the one predicted by most previous reconstructions, including for example the ICE-4G model by Peltier (1994), and the model results for the Eurasian Ice Sheet at the LGM by Siegert *et al.* (2001) and Siegert & Dowdeswell (2004). Our modeled ice surface elevation is in good agreement with the regional ice model results of Näslund *et al.* (2003), who studied ice-flow directions and erosion of the Fennoscandian Ice Sheet through time and obtained LGM surface elevations of *c.* 1750 to 250 m a.s.l. for our study area.

The relatively thin ice sheet that is predicted by our model also has important implications for determining the circumstances of sea level history during the last glacial–interglacial cycle. An imbalance exists between the global estimates of ice volumes inferred, for example, from coral records (e.g. Fairbanks 1989; Bard *et al.* 1990) and the sum of the individual ice-sheet volumes inferred from glacial rebound history (Lambeck *et al.* 2000). Our results, admittedly based on a single flowline, contradict Lambeck *et al.*'s hypothesis that a very thick Scandinavian Ice Sheet may have been responsible for a greater part of sea level rise after

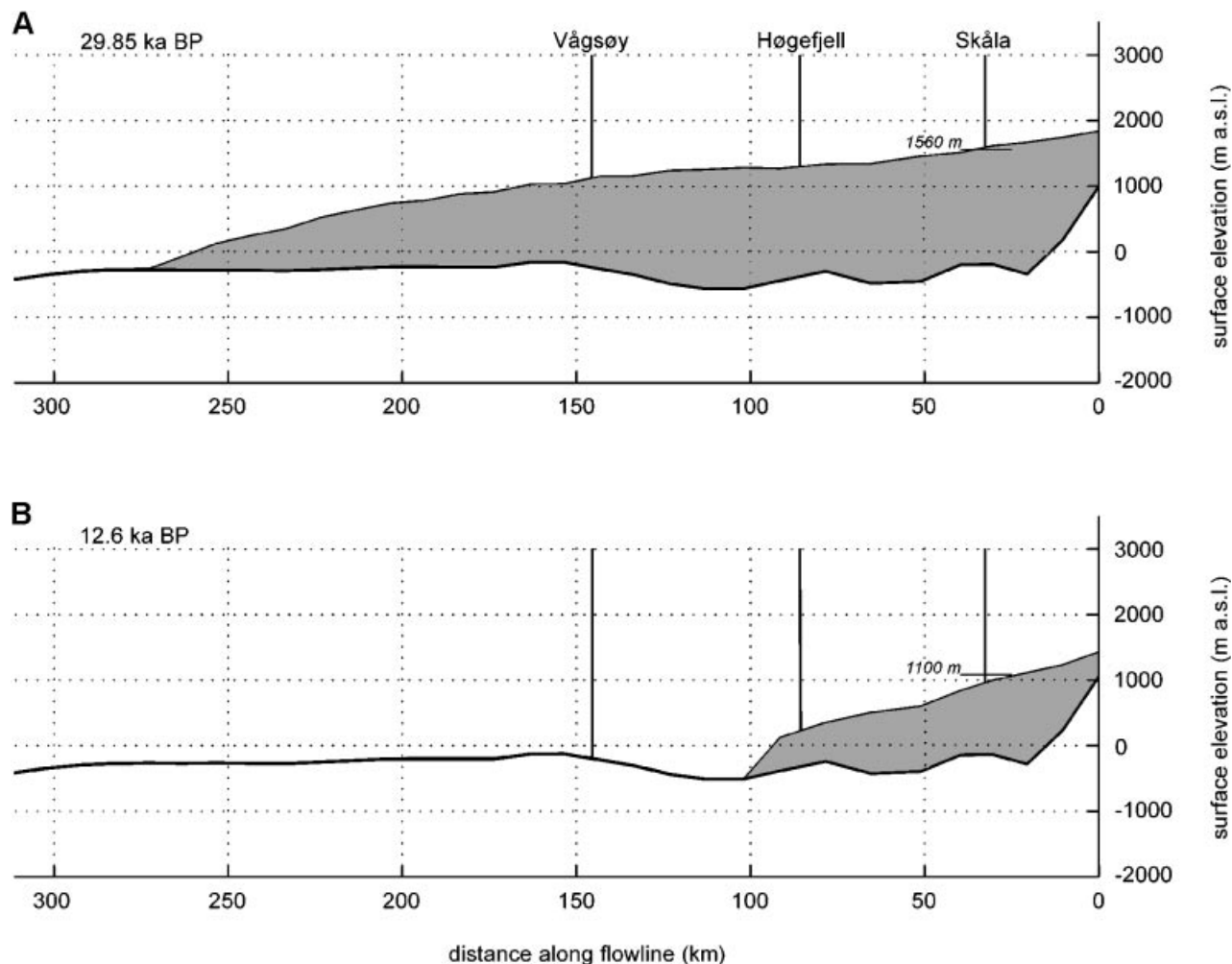


Fig. 4. Ice-sheet profiles along flowline from the standard experiment for the times corresponding to the maximum ice extent (A) and to the Younger Dryas readvance (B). The locations of Skåla, Høgefjell and Vågsøy are indicated for comparison of cosmogenic data with model results. Trimlines at Skåla identified in the field (Nesje *et al.* 1988) are marked with horizontal lines.

the last glaciation. The timing of the start of rapid deglaciation in our model results coincides well with the onset of major deglaciation at 14.2 ka BP inferred from an isochron map of the European ice sheet by Boulton *et al.* (2001) which is based on satellite images in combination with field observations.

Conclusions

Our numerical experiments with a time-dependent ice-flow model investigate the growth and shrinkage of glacier ice along a flowline of the southwestern Scandinavian Ice Sheet during the Late Weichselian. Paleoclimate input was varied within a reasonable range (based on GCM results and local proxy data). Based on comparison of our modeled ice extents along the flowline with field evidence, using the GISP2 $\delta^{18}\text{O}$ record as a paleotemperature proxy seems to be a

reasonable approach. All experiments yield ice thicknesses during the maximum glaciation that are lower than the highest mountain peaks in the area. If a water film developed beneath the ice, which seems likely according to ongoing studies using a groundwater flow model, it may have triggered fast ice flow, and ice profile gradients may have been even lower than modeled. Our model results therefore strongly support the theory of a relatively thin ice sheet that did not cover all the mountain peaks in western Norway at its last maximum extent.

Acknowledgements. – We thank A. Nesje and an anonymous referee for their constructive comments on the manuscript. Ed Brook and Henriette Linge made available unpublished cosmogenic data for comparison with our model results. Øyvind Nordli from the Norwegian Meteorological Institute provided the present-day climatology for the study area. This research was funded by NSF grant EAR-0087369 (C. Winguth, D. Mickelson, J. Darter and C. Moeller) and the Norwegian Research Council through the NORPAST project (E. Larsen).

References

- Andersen, B. G. 1981: Late Weichselian ice sheets in Europe. In Denton, G. H. & Hughes, T. J. (eds.): *The Last Great Ice Sheets*, 20–27. John Wiley & Sons, New York.
- Bard, E., Hamelin, B., Fairbanks, R. G. & Zindler, A. 1990: Calibration of the ^{14}C timescale over the past 30,000 years using mass spectrometric U-Th ages from Barbados corals. *Nature* 345, 405–410.
- Beck, J. W., Richards, D. A., Edwards, R. L., Silverman, B. W., Smart, P. L., Donahue, D. J., Herrera-Osterheld, S., Burr, G. S., Calsoyas, L., Jull, A. J. T. & Biddulph, D. 2001: Extremely large variations of atmospheric ^{14}C concentration during the last glacial period. *Science* 292, 2453–2458.
- Birks, H. H., Battarbee, R. W., Birks, H. J. B., Bradshaw, E. G., Brooks, S. J., Duigan, C. A., Jones, V. J., Lemdahl, G., Peglar, S. M., Solem, J. O., Solhøy, T. & Stalsberg, M. K. 2000: The development of the aquatic ecosystem at Kråkenes Lake, western Norway, during the late-glacial and early-Holocene – a synthesis. *Journal of Paleolimnology* 23, 91–114.
- Bond, G., Broecker, W., Johnson, S., McManus, J., Labeyrie, L., Jouzel, J. & Bonani, G. 1993: Correlations between climate records from North Atlantic sediments and Greenland ice. *Nature* 365, 143–147.
- Boulton, G. S., Dongelmans, P., Punkari, M. & Broadgate, M. 2001: Paleoglaciology of an ice sheet through a glacial cycle: the European ice sheet through the Weichselian. *Quaternary Science Reviews* 20, 591–625.
- Boulton, G. S. & Payne, A. 1994: Mid-latitude ice sheets through the last glacial cycle: glaciological and geological reconstructions. In Duplessy, J.-C. et al. (eds.): *Long-term Climatic Change: Data and Modeling*, 177–212. NATO Advanced Science Institutes Series I, Global Environmental Change 22. Springer, Berlin and Heidelberg.
- Boulton, G. S., Smith, G. O., Jones, A. S. & Newson, J. 1985: Glacial geology and glaciology of the last mid-latitude ice sheets. *Journal of the Geological Society of London* 142, 447–474.
- Brook, E. J., Nesje, A., Lehman, S. J., Raisbeck, G. M. & Yiou, F. 1996: Cosmogenic nuclide exposure ages along a vertical transect in western Norway: implications for the height of the Fennoscandian ice sheet. *Geology* 24, 207–210.
- Clark, P. U., Alley, R. B. & Pollard, D. 1999: Northern hemisphere ice-sheet influences on global climate change. *Science* 286, 1104–1111.
- Cuffey, K. M. & Clow, G. D. 1997: Temperature, accumulation, and ice sheet elevation in central Greenland through the last deglacial transition. *Journal of Geophysical Research* 102(C12), 26383–26396.
- Cutler, P. M., MacAyeal, D. R., Mickelson, D. M., Parizek, B. & Colgan, P. M. 2000: Numerical simulation of ice-flow-permafrost interactions around the southern Laurentide Ice Sheet. *Journal of Glaciology* 46, 311–325.
- Cutler, P. M., Mickelson, D. M., Colgan, P. M., MacAyeal, D. R. & Parizek, B. R. 2001: Influence of the Great Lakes on the dynamics of the southern Laurentide Ice Sheet: numerical experiments. *Geology* 29, 1039–1042.
- Dahl, S. O. & Nesje, A. 1992: Paleoclimate implications based on equilibrium-line altitude depressions of reconstructed Younger Dryas and Holocene cirque glaciers in inner Nordfjord, western Norway. *Palaeogeography, Palaeoclimatology, Palaeoecology* 94, 87–97.
- Donner, J. 1995: *The Quaternary History of Scandinavia*. 200 pp. Cambridge University Press, Cambridge.
- Fairbanks, R. G. 1989: A 17,000-year glacio-eustatic sea level record: influence of glacial melting rates on the Younger Dryas event and deep-ocean circulation. *Nature* 342, 637–642.
- Fareth, O. W. 1987: Glacial geology of Middle and Inner Nordfjord, western Norway. *Norges Geologiske Undersøkelse Bulletin* 408, 1–55.
- Follestad, B. A. 1990: Block fields, ice-flow directions and the Pleistocene ice sheet in Nordmøre and Romsdal, west Norway. *Norsk Geologisk Tidsskrift* 70, 27–33.
- Fronval, T., Jansen, E., Bloemendal, J. & Johnsen, S. 1995: Oceanic evidence for coherent fluctuations in Fennoscandian and Laurentide ice sheets on millennium timescale. *Nature* 374, 443–446.
- Ganopolski, A., Rahmstorf, S., Petoukhov, V. & Claussen, M. 1998: Simulation of modern and glacial climates with a coupled global model of intermediate complexity. *Nature* 391, 351–356.
- Greve, R. & MacAyeal, D. R. 1996: Dynamic/thermodynamic simulations of Laurentide ice-sheet instability. *Annals of Glaciology* 23, 328–335.
- Grootes, P. M. & Stuiver, M. 1997: Oxygen 18/16 variability in Greenland snow and ice with 10^3 to 10^5 -year time resolution. *Journal of Geophysical Research* 102, 26455–26470.
- Hafidason, H., Sejrup, H. P., Klitgaard, D. & Johnsen, S. 1995: Coupled response of the late glacial climate shifts of NW-Europe reflected in Greenland ice cores: evidence from the northern North Sea. *Geology* 23, 1059–1063.
- Heikkilä, M. & Seppä, H. 2003: A 11,000 yr paleotemperature reconstruction from the southern boreal zone in Finland. *Quaternary Science Reviews* 22, 541–554.
- Hildreth, M. 2001: *Surficial Geology and Late Weichselian Ice Sheet Thickness at Skorgedalen, Western Norway*. M.Sc. thesis, University of Wisconsin-Madison, 73 pp.
- Hooke, R. LeB. 1998: *Principles of Glacial Mechanics*. 248 pp. Prentice Hall, New Jersey.
- Hughes, T. J., Denton, G. H., Anderson, B., Schilling, D., Fastook, J. & Lingle, C. 1981: The last great ice sheets: a global view. In Denton, G. H. & Hughes, T. J. (eds.): *The Last Great Ice Sheets*, 275–318. John Wiley & Sons, New York.
- Huybrechts, P. & T'siobbel, S. 1995: Thermomechanical modeling of Northern Hemisphere ice sheets with a two-level mass-balance parameterization. *Annals of Glaciology* 21, 111–116.
- Imbrie, J., Hays, J. D., Martinson, D. G., McIntyre, A., Mix, A. C., Morlet, J. J., Pisias, N. G., Prell, W. L. & Shackleton, N. J. 1984: The orbital theory of Pleistocene climate: support from a revised chronology of the marine $\delta^{18}\text{O}$ record. In Berger, A. L. et al. (eds.): *Milankovitch and Climate, Part 1*, 269–305. Reidel Publication Company, Higham.
- Kildal, E. 1970: Florø. Bedrock map 1 : 250 000. Geological Survey of Norway.
- Kleman, J. & Hättestrand, C. 1999: Frozen-bed Fennoscandian and Laurentide ice sheets during the last glacial maximum. *Nature* 402, 63–66.
- Kleman, J., Hättestrand, C. & Clarhäll, A. 1999: Zooming in on frozen-bed patches: scale-dependant controls on Fennoscandian ice sheet basal thermal zonation. *Annals of Glaciology* 28, 189–194.
- Kukkonen, I. T., Gosnold, W. D. & Safanda, J. 1998: Anomalously low heat flow density in eastern Karelia, Baltic Shield: a possible paleoclimatic signature. *Tectonophysics* 291, 235–249.
- Kutzbach, J., Gallimore, R., Harrison, S., Behling, P., Selin, R. & Laarif, F. 1998: Climate and biome simulations for the past 21,000 years. *Quaternary Science Reviews* 17, 473–506.
- Lambeck, K., Yokoyama, Y., Johnston, P. & Purcell, A. 2000: Global ice volumes at the Last Glacial Maximum and early Lateglacial. *Earth and Planetary Science Letters* 181, 513–527.
- Larsen, E., Gulliksen, S., Lauritzen, S.-E., Lie, R., Løvlie, R. & Mangerud, J. 1987: Cave stratigraphy in western Norway; multiple Weichselian glaciations and interstadial vertebrate fauna. *Boreas* 16, 267–292.
- Larsen, E., Lyså, A., Demidov, I., Funda, S., Houmark-Nielsen, M., Kjær, K. H. & Murray, A. S. 1999: Age and extent of the Scandinavian ice sheet in northwest Russia. *Boreas* 28, 115–132.
- Larsen, E., Sandven, R., Heyerdahl, H. & Hernes, S. 1995: Glacial geological implications of preconsolidation values in sub-till sediments at Skorgenes, western Norway. *Boreas* 24, 37–46.
- Larsen, E. & Stalsberg, M. K. 2004: Younger Dryas glaciolacustrine rhythmites and cirque glacier variations at Kråkenes, western

- Norway: depositional processes and climate. *Journal of Paleolimnology* 31, 49–61.
- Lutro, O. 1997: Årdal. Bedrock map 1 : 250 000. Geological Survey of Norway.
- Manabe, S. & Broccoli, A. J. 1985: The influence of continental ice sheets on the climate of an ice age. *Journal of Geophysical Research* 90, 2167–2190.
- McCarroll, D. & Nesje, A. 1993: The vertical extent of ice sheets in Nordfjord, western Norway: measuring degree of rock surface weathering. *Boreas* 22, 255–265.
- Moeller, C. 2004: *Modeling the groundwater flow system along a flow line of the Scandinavian Ice Sheet*. M.Sc. thesis, University of Wisconsin-Madison, 61 pp.
- Näslund, J. O., Rodhe, L., Fastook, J. L. & Holmlund, P. 2003: New ways of studying ice sheet flow directions and glacial erosion by computer modelling – examples from Fennoscandia. *Quaternary Science Reviews* 22, 245–258.
- Nesje, A. & Dahl, S. O. 1990: Autochthonous block fields in southern Norway: implications for the geometry, thickness, and isostatic loading of the Late Weichselian Scandinavian ice sheet. *Journal of Quaternary Science* 5, 225–234.
- Nesje, A., Anda, E., Rye, N., Lien, R., Hole, P. A. & Blikra, L. H. 1987: The vertical extent of the Late Weichselian ice sheet in the Nordfjord–More area, western Norway. *Norsk Geologisk Tidsskrift* 67, 125–141.
- Nesje, A., Dahl, S. O., Anda, E. & Rye, N. 1988: Block fields in southern Norway: significance for the Late Weichselian ice sheet. *Norsk Geologisk Tidsskrift* 68, 149–169.
- Nesje, A., Dahl, S. O., Valen, V. & Øvstedal, J. 1992: Quaternary erosion in the Sognefjord drainage basin, western Norway. *Geomorphology* 5, 511–520.
- Nygård, A., Sejrup, H. P., Hafidason, H., Cecchi, M. & Ottesen, D. 2004: Deglaciation history of the southwestern Fennoscandian Ice Sheet between 15 and 13 ¹⁴C ka BP. *Boreas* 33, 1–17.
- Oerlemans, J. 1981: Modelling of Pleistocene European ice sheets: some experiments with simple mass-balance parameterizations. *Quaternary Research* 15, 77–85.
- Parizek, B. R. 2000: *Thermomechanical Flowline Model for Studying the Interaction between Ice Sheets and the Global Climate System*. M.Sc. thesis, Pennsylvania State University, 150 pp.
- Paterson, W. S. B. 1994: *The Physics of Glaciers*. 481 pp. Butterworth-Heinemann, Oxford.
- Payne, A. J. 1995: Limit cycles in the basal thermal regime of ice sheets. *Journal of Geophysical Research* 100(B3), 4249–4263.
- Peltier, W. R. 1994: Ice age paleotopography. *Science* 265, 195–201.
- Pelto, M. S. & Warren, C. R. 1991: Relationship between tidewater glacier calving velocity and water depth at the calving front. *Annals of Glaciology* 15, 115–118.
- Renssen, H., Isarin, R. F. B., Jacob, D., Podzun, R. & Vandenberghe, J. 2001: Simulation of the Younger Dryas climate in Europe using a regional climate model nested in an AGCM: preliminary results. *Global and Planetary Change* 30, 41–57.
- Riis, F. 1996: Quantification of Cenozoic vertical movements of Scandinavia by correlation of morphological surfaces with offshore data. *Global and Planetary Change* 12, 331–357.
- Sejrup, H. P., Aarseth, I. & Hafidason, H. 1991: The Quaternary succession in the northern North Sea. *Marine Geology* 101, 103–111.
- Sejrup, H. P., Hafidason, H., Aarseth, I., King, E., Forsberg, C. F., Long, D. & Rokoengen, K. 1994: Late Weichselian glaciation history of the northern North Sea. *Boreas* 23, 1–13.
- Sejrup, H. P., Larsen, E., Landvik, J., King, E. L., Hafidason, H. & Nesje, A. 2000: Quaternary glaciations in southern Fennoscandia: evidence from southwestern Norway and the northern North Sea region. *Quaternary Science Reviews* 19, 667–685.
- Shin, S.-I., Liu, Z., Otto-Bliesner, B., Brady, E. C., Kutzbach, J. E. & Harrison, S. P. 2003: A simulation of the Last Glacial Maximum climate using the NCAR-CCSM. *Climate Dynamics* 20, 127–151.
- Siegert, M. J. & Dowdeswell, J. A. 2004: Numerical reconstructions of the Eurasian Ice Sheet and climate during the Late Weichselian. *Quaternary Science Reviews* 23, 1273–1283.
- Siegert, M. J., Dowdeswell, J. A., Hald, M. & Svendsen, J.-I. 2001: Modelling the Eurasian Ice Sheet through a full (Weichselian) glacial cycle. *Global and Planetary Change* 31, 367–385.
- Sollid, J. L. & Sørbel, L. 1994: Distribution of glacial landforms in southern Norway in relation to the thermal regime of the last continental ice sheet. *Geografiska Annaler* 76A, 25–35.
- Stuiver, M., Reimer, P. J., Bard, E., Beck, J. W., Burr, G. S., Hughen, K. A., Kromer, B., McCormac, G., van der Plicht, J. & Spurk, M. 1998: INTCAL98 Radiocarbon age calibration, 24,000–0 cal BP. *Radiocarbon* 40, 1041–1083.
- Svendsen, J. I., Astakhov, V. I., Bolshiyakov, D. Yu., Demidov, I., Dowdeswell, J. A., Gataullin, V., Hjort, C., Hubberten, H. W., Larsen, E., Mangerud, J., Melles, M., Möller, P., Saarnisto, M. & Siegert, M. J. 1999: Maximum extent of the Eurasian ice sheets in the Barents and Kara Sea region during the Weichselian. *Boreas* 28, 234–242.
- Valen, V., Mangerud, J., Larsen, E. & Hufthammer, A. K. 1996: Sedimentology and stratigraphy in the cave Hamnsundhelleren, western Norway. *Journal of Quaternary Sciences* 11, 185–201.
- Winguth, C., Mickelson, D. M., Colgan, P. M. & Laabs, B. J. C. 2004: Modeling the deglaciation of the Green Bay Lobe of the southern Laurentide Ice Sheet. *Boreas* 33, 34–47.